J Appl Electrochem (2014) 44:215–224
DOI 10.1007/s10800-013-0618-2

RESEARCH ARTICLE

Carbon-supported Pt(Cu) electrocatalysts for methanol oxidation prepared by Cu electroless deposition and its galvanic replacement by Pt

J. Georgieva · E. Valova · I. Mintsouli · S. Sotiropoulos · S. Armyanov · A. Kakaroglou · A. Hubin · O. Steenhaut · J. Dille

Received: 3 June 2013 / Accepted: 18 August 2013 / Published online: 27 August 2013

Abstract Bimetallic Pt–Cu carbon-supported catalysts (Pt(Cu)/C) were prepared by electroless deposition of Cu on a high surface area carbon powder support, followed by its partial exchange for Pt; the latter was achieved by a galvanic replacement process involving treatment of the Cu/C precursor with a chloroplatinate solution. X-ray diffraction characterization of the Pt(Cu)/C material showed the formation of Pt-rich Pt–Cu alloys. X-ray photoelectron spectroscopy revealed that the outer layers are mainly composed of Pt and residual Cu oxides, while metallic Cu is recessed into the core of the particles. Repetitive cyclic voltammetry in deaerated acid solutions in the potential range between hydrogen and oxygen evolution resulted in steady-state characteristics similar to those of pure Pt, indicating the removal of residual Cu compounds from the surface (due to electrochemical treatment) and the formation of a compact Pt outer shell. The electrocatalytic activity of the thus prepared Pt(Cu)/C material toward methanol oxidation was compared to that of a commercial Pt/C catalyst as well as of similar Pt(Cu)/C catalysts formed by simple Cu chemical reduction. The Pt(Cu)/C catalyst prepared using Cu electroless plating showed more pronounced intrinsic catalytic activity toward methanol oxidation than its counterparts and a similar mass activity when compared to the commercial catalyst. The observed trends were interpreted by interplay between mere surface area effects and modification of Pt electrocatalytic performance in the presence of Cu, both with respect to methanol oxidation and poisonous CO removal.

Keywords Binary electrocatalysts · Electroless deposition · Galvanic replacement · Methanol oxidation

J. Georgieva (✉) · E. Valova · S. Armyanov
Rostislaw Kaischew Institute of Physical Chemistry, Bulgarian Academy of Sciences, 1113 Sofia, Bulgaria
e-mail: jenia@ipc.bas.bg

I. Mintsouli · S. Sotiropoulos
Department of Chemistry, Aristotle University of Thessaloniki, 54124 Thessaloníki, Greece

A. Kakaroglou · A. Hubin · O. Steenhaut
Department of Electrochemical and Surface Engineering, Vrije Universiteit Brussel, 1050 Brussels, Belgium

J. Dille
Service 4 MAT Materials, Engineering, Characterization, Synthesis and Recycling, Ecole Polytechnique de Bruxelles, 1050 Brussels, Belgium

1 Introduction

Direct methanol fuel cells (DMFCs) received much attention as a power source for potential applications, initially in hybrid electrical vehicles and more recently in portable electronic devices [1, 2]. Compared to hydrogen, the use of methanol as fuel has some advantages: it is cheaper, easily transported and stored while having a high theoretical energy density too [3, 4]. Two of the major problems limiting the DMFCs performance are their high price and low reaction rate of methanol oxidation at the anode [5, 6]. Another practical problem concerns its toxicity. Platinum is one of the best catalysts for methanol oxidation reaction (MOR) but, apart from its high cost and limited abundance, it is generally recognized that pure Pt at room or moderate temperatures is prone to poisoning by CO, an intermediate in the oxidation of methanol [7–9]. In the past decade, significant research efforts have been made in order to develop catalysts as anode materials with improved

catalytic activity for methanol oxidation, CO tolerance and reduced cost.

Although Pt–Ru alloys are still the most active catalysts for methanol oxidation, the high cost of Ru has led to search for other less expensive metals (e.g., Cu, Fe, Co, Ni, etc.) that exhibit enhancement of Pt or Pt–Ru catalytic activity. The promoting effect of the second metal may be explained on the basis of a bifunctional mechanism for CO oxidation (in which the CO poisoned Pt is regenerated via a surface reaction between CO and oxygenated species preferably formed on the other metal(s) to yield CO_2) or/and a modification of Pt electronic properties which, according to density function theory, should cause a downshift of the Pt d-band center, weakening the Pt–CO bond [10–13].

Various carbon-supported binary or ternary Pt-based metal catalysts for fuel cell reactions have been studied [7, 14–17]. Different methods for the preparation of the catalysts are used [15, 17]: impregnation of carbon support with metal precursors followed by reduction in the precursors with different reducing agents (either in liquid phase or in a reducing atmosphere at high temperatures) and adsorption of platinum and metal colloids onto the carbon surface. The colloids methods commonly used are the Bonnemann method [18] and polyol synthesis [19].

During the last decade, a new method for the introduction of the noble metal onto the electrode support has been developed. This method (also known as galvanic replacement or transmetallation) is based on spontaneous partial replacement of early transition metal layers (Cu, Fe, Ni, Co, etc.) by more noble metal (Pt, Pd, Ir, Au, etc.) through immersion of the samples into a solution containing the precious metal ions. It was first applied by Adzic et al. [20, 21] to underpotentially deposited (UPD) Cu monolayers and to Cu and Pb bulk deposits by Kokkinidis and coworkers [22, 23] on flat electrode substrates. The method has been further expanded by Sotiropoulos et al. to the replacement of electrodeposited Pb, Cu, Fe, Co and Ni polylayers by Pt and Au. Pt(M), Au(M) and PtAu(M) catalysts have been tested for fuel cell-related reactions including methanol oxidation [24–27].

Advantages of the new technique include the fact that it is a fast and room temperature process, employs low concentration solutions of the precious metal and can lead to the formation of thin precious metal deposits that may decrease its loading. In recent years, this method has been used as an alternative route for the preparation of practical catalysts, supported on high surface area carbon, mainly in search of efficient oxygen reduction electrocatalysts. There are only few papers dealing with such Pt(Cu)/C [28–32] and Pt(Ni)/C [33–35] catalysts for ethanol and methanol oxidation in acid. In general, the Pt-based Cu and Ni catalysts demonstrate comparable or enhanced electrocatalytic performance toward methanol oxidation in comparison with commercial Pt electrocatalyst. The catalytic activity for MOR at binary Pt-based systems depends in general on the second metal content, the degree of its alloying with Pt, morphology, structure and support material. It was found that the mechanism of formation and the properties of the catalyst are largely determined by the dispersion degree of the initial less noble metal deposit [31].

In a recent paper, we have synthesized Pt(Cu)/C catalysts, whereby the precursor Cu/C material was prepared by simple chemical reduction in Cu salts by $NaBH_4$ in slurries containing the C powder [32]. This crude approach resulted in large Cu particles (mostly many tens of nm large) and apparently poor adherence on C, as inferred by the large Cu losses (Cu that was etched without being platinized or contained on Pt(Cu) particles of loose adherence), that summed up to ca 72 %. Recently, seeking for an alternative method for precursor metal preparation, we have published results concerning the electrocatalytic activity toward methanol oxidation of Pt(Ni–P) carbon-supported (denoted as Pt(Ni)/C) catalysts, prepared by a combination of electroless deposition of low-P-content crystalline Ni on C and subsequent partial galvanic replacement of Ni by Pt [35]. Electroless deposition of crystalline Ni–P on C has been used as an alternative, low temperature method, favorable for more homogeneous distribution of Ni crystallites and their stronger adherence to carbon.

As a natural continuation of these studies, the aim of the current work has been the use of electroless deposition as an alternative method to deposit the Cu precursor on high surface area carbons and the study of methanol oxidation at the resulting Pt(Cu)/C catalyst prepared by transmetallation. The specific objectives have been (1) to prepare practical Pt(Cu)/C methanol oxidation catalysts by electroless deposition/transmetallation, (2) to compare the structure, morphology and composition of these Pt(Cu)/C materials with that of similar ones, whereby the precursor Cu was prepared by chemical reduction in solution and (3) to compare their electrocatalytic activity toward methanol oxidation with that of their above-mentioned counterparts as well as with a commercial Pt/C catalyst.

2 Experimental

2.1 Preparation of Pt(Cu)/C powder catalyst

The Pt(Cu)/C powder catalyst was prepared following the same two-step process of Pt(Ni)/C preparation, reported previously [35]. High surface area carbon powder support (Vulcan XC72R, Cabot) was subjected to an oxidative pretreatment [36]; 0.25 g of the carbon powder was

immersed in 100 ml solution of 1.0 M sulfuric acid (Merck, for analysis) and 10 g of ammonium persulfate (Merck, ACS reagent) at room temperature and stirred for 24 h using a magnetic stirrer. The suspension was filtered, and the precipitate was rinsed with H_2O and left to dry overnight. Before electroless deposition of Cu, 0.125 g of the oxidized carbon was activated in 50 ml of 0.1 M HCl (Aldrich) and 10^{-3} M $PdCl_2$ (anhydrous, 59 % Pd). The suspension was left for 30 min under magnetic stirring to ensure palladium ion adsorption on the carbon surface and filtered. The precipitate was rinsed with H_2O and left to dry overnight. The activated carbon powder was immersed in 100 ml of a solution for electroless copper deposition [37]. The bath composition was modified by reducing the concentration of Cu metal source in order to lower the content of Cu, deposited on carbon. The main components of the solution were 0.01 M $CuSO_4{\cdot}5H_2O$ as Cu metal source, 30 ml/l CH_2O (37 %) as a reducing agent, 0.05 M Na_2-EDTA as a complexing agent, as well as stabilizers, buffering compounds and surfactant. The bath temperature was 45 °C and solution pH within 12.5–13.0 range. The suspension was left for 30 min under magnetic stirring and filtered. The obtained Cu/C precipitate was rinsed with H_2O and left to dry in vacuum (1.5×10^{-3} Torr).

The as-prepared Cu/C powder precursor (0.127 g) was slowly added to 25 ml solution of 5×10^{-3} M K_2PtCl_6 salt (Sigma-Aldrich, ACS reagent, ≥37.50 % as Pt) in 0.1 M HCl (Aldrich) under continuous magnetic stirring for 30 min. Spontaneous Cu galvanic (partial) replacement by Pt occurs, as expected from the difference between the standard potential values E^0 of $[PtCl_6]^{2-}$/Pt (+0.744 V vs. NHE) and Cu^{2+}/Cu (+0.340 V vs. NHE) [38]. A symbolic notation of the transmetalation reaction could be written as:

$$(x\mathrm{Cu/C}) + y\mathrm{PtCl}_6^{2-} \rightarrow \mathrm{Pt}_y\mathrm{Cu}_{x-2y}/\mathrm{C} + 2y\mathrm{Cu}^{2+} + 6y\mathrm{Cl}^- \quad (1)$$

where $x \geq 2y$.

2.2 Microscopic, spectroscopic and crystallographic characterization

The morphology and structure of the catalysts were investigated with transmission electron microscopy (TEM) and selected area electron diffraction (SAED) coupled with EDS analysis using PHILIPS CM 20 UltraTwin at 200 kV.

Energy dispersive spectroscopic (EDS) elemental analysis was also carried out using a JEOL JSM 6390 microscope with INCA Oxford Energy 350 system.

X-ray diffraction (XRD) characterization of the catalysts was made with the help of Bruker Diffractometer D5000 (Cu anode 40 kV, 40 mA) using Cu Ka-filtered radiation 1.5406 Å, Step 0.02° 2θ, time per step 3 s.

X-ray photoelectron spectroscopy (XPS) study was performed in a PHI 5600 (Physical Electronics) XPS spectrometer using the monochromatic Al Kα line 1,486.6 eV at 300.0 W. The binding energies were calibrated according to ISO 15472 requirements measuring three peaks: low (Au 4*f*7/2), medium (Ag 3*d*5/2) and high binding energy peaks (Cu 2*p*3/2). In high resolution experiments, the increment was 0.05 eV. The PHI Multipak 9.3 software was used for data interpretation.

2.3 Electrode preparation and electrochemical characterization

In order to test and compare the electrochemical behavior of the Pt(Cu)/C with respect to commercial 20 % w/w Pt/C catalyst, ETEK, 3 mg of each material was dispersed ultrasonically in 0.75 ml H_2O and 1.5 ml from a mixture of 4.85 ml ethanol and 0.15 ml Nafion® (5 % w/w solution, Aldrich). A given quantity of the slurry, containing 1.0–1.2 mg supported catalyst, was transferred onto a flat glassy carbon electrode (GC, BAS Inc.) using a pipette and left to dry. The geometric area of the electrode was 0.385 cm^2. The total catalyst loading was in the 2.6–3.1 mg cm^{-2} range. The weight of the added polymer and catalyst was determined with the help of an electronic balance, during parallel additions of the corresponding suspension on an aluminum foil until solvent evaporation was complete and no further weight change was observed. Based on the EDS analysis of the catalysts, the Pt loading for the electrodes whose results are presented below was 0.5 mg cm^{-2} for both the Pt(Cu)/C and the Pt/C ETEK catalysts.

The electrochemical measurements were performed with the Autolab 100 (EcoChemie) system. Cyclic voltammetric (CV) experiments were carried out in a three-compartment cell with the reference and counter electrode chambers, separated from the working electrode by a Luggin capillary and a glass frit, respectively. A Pt wire was used as the counter electrode and a saturated calomel electrode (SCE; Radiometer) as the reference electrode.

The electrodes were first scanned repeatedly in a nitrogen deaerated 0.1 M $HClO_4$ between the hydrogen and oxygen evolution potential limits at 1 V s^{-1} and 50 mV s^{-1} to dissolve anodically any uncovered Cu. As a result, steady-state voltammograms, comparable to Pt, were obtained. To evaluate the catalytic activity of the catalysts toward CO oxidation, the electrodes were put in a clean deaerated 0.1 M $HClO_4$, saturated with pure CO gas (>99.99 % purity; Air Liquid). The electrodes were held at +0.10 V versus SCE for 5 min, allowing for CO adsorption, before being scanned to more positive potentials at a 50 mV s^{-1} potential scan rate, for CO monolayer oxidation. Then, the solution was replaced by a 0.1 M

$HClO_4$ + 0.5 M methanol (MeOH) deaerated solution (Riedel; puriss p.a., ACS reagent, ≥70 % and Chromasolv® for HPLC, gradient grade, ≥99.9 %, respectively), and the electrodes were swept at a scanning rate of 5 mV s^{-1} between +0.10 and +0.80 V versus SCE, until steady-state pictures were obtained.

3 Results and discussion

3.1 Microscopic, crystallographic and spectroscopic characterization

Figure 1a–c presents the TEM micrographs of the Cu/C precursor (a), the Pt(Cu)/C catalyst (b) and the commercial Pt/C ETEK (c) catalyst. The carbon support consists of 30–40 nm spherical particles, aggregated in chainlike structures.

The electrolessly deposited Cu particles, seen as black spots in Fig. 1a, appeared organized in a variety of sizes (from a few tens of nm up to (rarely) 50 nm aggregates) on top of C particles. Despite the fact that their density varied depending on location (results for other locations not shown here), they never exceeded 50 nm, unlike the chemically produced Cu particles of [32] which were larger and, apparently, loosely connected to the C support.

The individual Pt(Cu) particles seen in Fig. 1b appear to be spheroidal with diameter ca. 3 nm. However, in contrast to the Pt/C reference in Fig. 1c, they are organized in aggregates of irregular shapes a few to tens of nm large, i.e., bigger than those of [32] that were produced from the platinization of chemically deposited larger particles. This may be due to the fact that in the latter case, any Pt directly deposited on large Cu particles is likely to collapse together with its support, whereas only Pt films formed on small Cu particles or pure Pt nuclei deposited at nearby C locations are likely to be stable; if Pt nuclei outnumber Pt(Cu), then smaller Pt particles are expected. On the contrary, in the case of Pt deposition on small, electrolessly produced Cu particles, a complete Pt protective shell is formed over Cu cores firmly attached onto carbon; if these are stable and form the majority of deposited Pt particles, then the latter are expected to be larger. Also, although the bimetallic Pt(Cu) particles of this work are homogeneously dispersed on the surface of the carbon support, they show a tendency to form aggregates which may result from the size and distribution of the precursor Cu particles where Pt preferentially deposits. On the other hand, the particles of the commercial Pt/C reference catalyst (Fig. 1c) are well dispersed and have a size of approximately 2 nm and no tendency to aggregate. The selected area electron diffraction (SAED) ring patterns presented in the insets of the

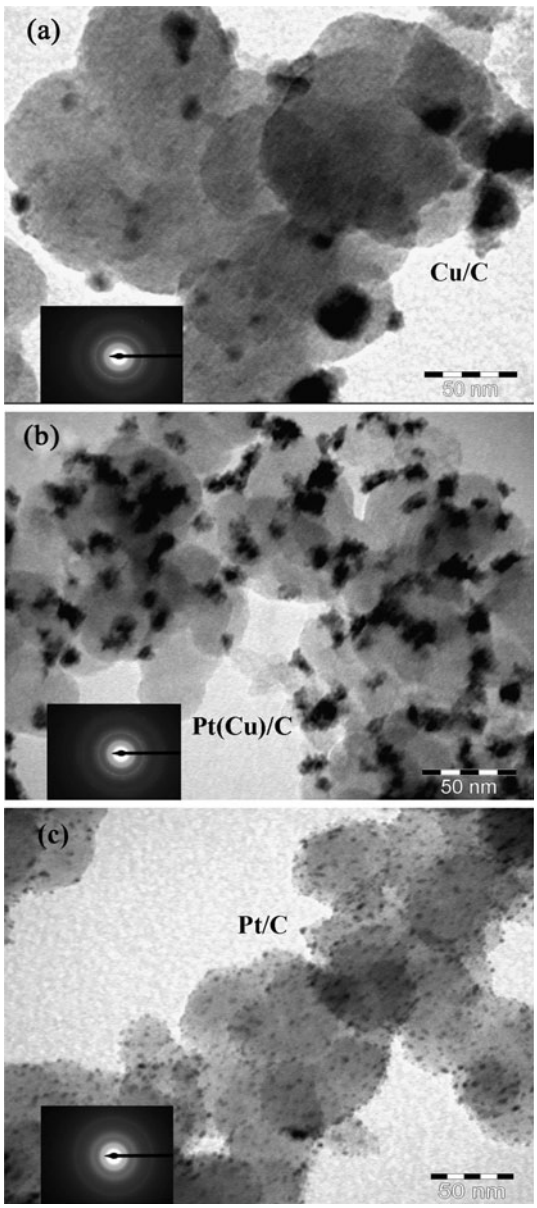

Fig. 1 TEM micrographs and SAED images of Cu/C (**a**), Pt(Cu)/C (**b**) and Pt/C ETEK (**c**) supported catalyst particles

Fig. 1a–c are characteristic of polycrystalline nanoparticulate materials.

EDS elemental analysis of the Cu/C precursor and the Pt(Cu)/C catalyst is presented in Table 1. The errors correspond to 2σ values estimated by standardless analysis based on internal standards included in the software of INCA Oxford Energy 350 system. It is seen that the Pt(Cu) material originating from electroless Cu contains Pt at levels found in commercial catalysts (18.5 % w/w) and significant quantity of Cu too (7.9 % w/w); this should be contrasted to the much smaller Pt quantity (9.5 %) and insignificant amount of Cu (2.7 %) contained in similar catalysts originating from chemically deposited Cu [32].

Table 1 EDS results of Cu/C precursor and Pt(Cu)/C catalyst

Element Line	Cu/C			Pt(Cu)/C		
	Weight %	Error	Atomic %	Weight %	Error	Atomic %
C K	72.5	±0.65	91.7	70.5	±0.67	91.4
O K	2.4	±0.31	2.3	3.1	±0.32	3.1
Cu K	25.1	±0.6	6.0	7.9	±0.4	2.0
Pt M	–	–	–	18.5	±0.55	1.5
Total	100			100		

The relative atomic composition of Pt and Cu is, however, 43 at.% Pt ÷ 57 at.% Cu, very similar to that of [32] (44 at.% Pt ÷ 56 at.% Cu). The weight percentage of Cu in the precursor Cu/C material (25.1 %) is consistent with complete reduction in Cu(II) from the electroless deposition bath. However, the Cu content becomes significantly lower (7.9 % w/w) after immersion of the precursor Cu/C in the chloroplatinate solution. This is due to Cu dissolution by corrosion processes competitive to transmetalation; these can take place in the acidic aerated solution of catalyst preparation especially when the low Pt complex concentration (5×10^{-3} M) becomes depleted. Nevertheless, taking into account the initial Cu content, the 2Cu ÷ 1Pt stoichiometry of reaction (1) and the Cu content in the platinized material, we can calculate that 32 % of initial Cu remained in the bimetallic catalyst, 50 % has been exchanged for Pt, while only 18 % has been dissolved by competitive corrosion processes ("lost"). This constitutes a major improvement to the ca 72 % losses observed in the case of chemically reduced Cu precursors [32]. This effect can again be attributed to the smaller and well adhered to the support Cu precursor particles that are faster to be covered by a thin protective Pt layer.

Figure 2 displays the XRD pattern of Cu/C precursor and Pt(Cu)/C particles. The peaks in Fig. 2a were indexed to FCC lattice and associated with Cu(111), (200), (220) and (222) correspondingly. The additional small peaks were ascribed to Cu_2O showing the natural surface oxidation of the precursor. One may expect some small amount of CuO also which is either amorphous or of insufficient quantity to be displayed by XRD. This is linked to Cu/C exposure to ambient air during and after preparation. It can be estimated that the XRD pattern of the precursor Cu/C particles corresponds to larger mean crystallite size, showing sharper peaks with higher intensity than the Pt(Cu)/C. The particle size calculations were made using the Scherrer equation (see for example [39]:

$$t = K\lambda/\mathrm{B}\cos\theta_{\mathrm{B}},$$

where $K = 0.9$, λ is the wavelength of the X-ray radiation, B is the width (in radians) of the measured diffraction line at an intensity equal to half the maximum intensity (FWHM) and θ_B is the Bragg angle.

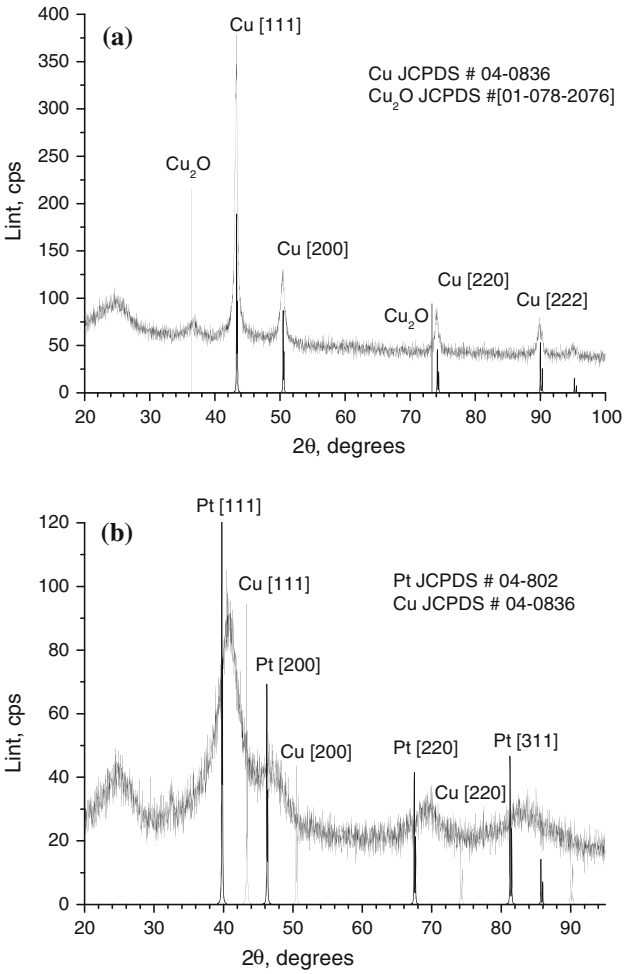

Fig. 2 XRD patterns of: (**a**) Cu/C precursor; (**b**) Pt(Cu)/C nanocatalysts. The reference data are marked according to the following JCPDS files: Cu 04-0836; Cu_2O 01-078-2076; Pt 04-802

In this case, the lines at $2\theta_{111} = 43.4$ of the XRD diagram of Cu/C and $2\theta_{111} = 40.8$ of Pt(Cu)/C were measured as the sharpest ones. The calculated mean particle sizes were 14 nm for the Cu/C precursor and 4 nm for the nanocatalyst Pt(Cu)/C. This is a good correspondence with the TEM observations.

The diffraction diagram of Pt(Cu)/C only shows a unique FCC phase with peaks shifted to higher reflection angles in respect of pure Pt (Fig. 2b). This points out that

the bulk composite material Pt(Cu)/C contains a Pt–Cu alloy. Bearing in mind that due to the small particle size, the diffraction lines are broad and weak, the interplanar spacings have been calculated for lines that were well defined, after suitable peak profile approximation and peak position determination. High precision determination of unit cell parameter needs a number of distinct sharp peaks at Bragg angles as high as possible. Since unfortunately this is not the case, [111], [220] and [311] lines have been used for calculations. The obtained values were put against $\cos^2\theta$ and through linear extrapolation toward $\cos^2\theta = 0$ the resulting value was taken as the unit cell parameter [39]. Application of the Vegard's law (i.e., linear dependence of the unit cell parameter on alloying metal concentration) gives the composition of ~70 at.% Pt and ~30 at.% Cu (a slightly more Pt-rich alloy than that of [32] whose composition was estimated as 63–37 %, respectively). The excess of Pt in the alloy (70 at.% as estimated by XRD) and the slight excess of Cu in the material as a whole (57 at.%) implies the presence of un-alloyed Cu in the particles which should, however, be of a size so small as not to be detected as discrete XRD peaks. No XRD peaks of Cu oxides are present after the transmetallation, meaning Cu is predominantly in metallic state in the bulk of the nanocatalyst and indicating an effective surface replacement of Cu by Pt.

From the XPS Cu 2*p* spectrum shown in Fig. 3a, one may conclude that on the surface layers of the precursor the presence of Cu(0) and Cu(I) are dominating (~75 %) over that of Cu(II) (~25 %). These values are obtained by curve fitting and evaluation of the ratios of the peak areas after deconvolution. From peaks 1(Cu(0) + Cu(I)) and 2 + 3 + 4 (Cu(II) + satellites), it is calculated Cu + Cu(I) ≈ 75 %, therefore: Cu(II) ≈ 25 %.

It is hard to estimate the ratio Cu(I)/Cu(0) without special investigations enabling the correct introduction of Auger parameter as it was done in [40]. The approximate evaluation of this parameter using surface survey data indicates that at the precursor surface, Cu(I) dominates over Cu(0) which is logical and in accordance with its detectability and presence in the XRD patterns. Therefore, at the precursor surface, one may expect Cu(I) > Cu(0) > Cu(II).

Comparing the XPS Cu 2*p* spectra of the Cu/C precursor and Pt(Cu)/C nanocatalyst in Fig. 3a, b, respectively, one may notice that the intensity is lower and the noise higher in the case of the Pt(Cu)/C spectrum. This is to be expected since the platinization of the precursor results in a significant decrease in Cu content due to both its exchange by Pt and its loss by competitive corrosion processes (see Discussion above). In addition, the satellite peaks' appearance in the 939–942 eV range is prominent in the case of Pt(Cu)/C indicating the Cu(II) prevails in the platinized material. Calculations of the content of Cu and Cu oxides

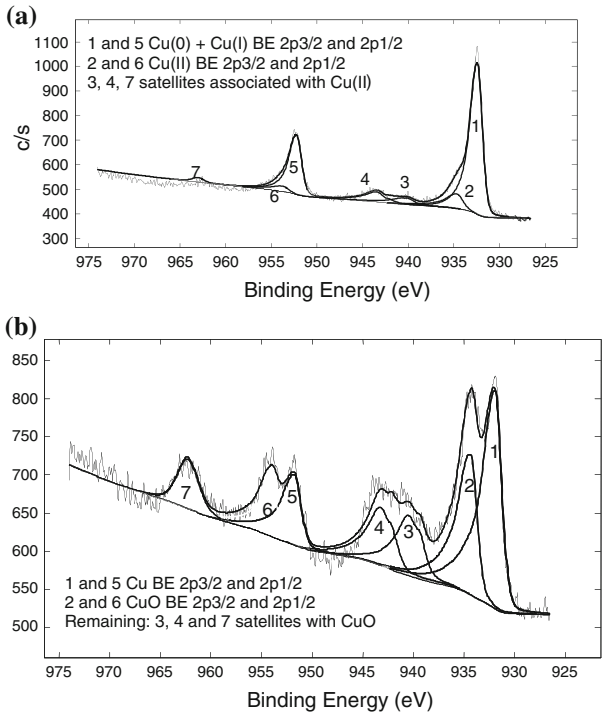

Fig. 3 XPS spectra in Cu 2*p* BE region of: (**a**) the catalyst precursor: electroless Cu on carbon powder; (**b**) Pt(Cu)/C nanocatalyst prepared by galvanic replacement. After the deconvolution, the peaks 1 and 5 are associated with Cu + Cu_2O (reference data for Cu BE: $2p_{3/2}$ 932.4 eV; $2p_{1/2}$ 952.2) and 2 and 6 with CuO (reference data for CuO BE: $2p_{3/2}$ 933.6; $2p_{1/2}$ 953.6). The satellite peaks are attributed to CuO

are similar as in the case of the precursor: from peaks 1(Cu(0) + Cu(I)) and 2 + 3+4 (Cu(II) + satellites) Cu + Cu(I) ≈ 43 %, therefore: Cu(II) ≈ 57 %. These observations can be explained by replacement of Cu(0) and Cu(I) by Pt from the precursor surface and their oxidation to soluble Cu^{++} ions. On the contrary, Cu(II) present on the surface cannot be further oxidized and remains a surface passivation layer (undetectable by XRD and expected to be anodically dissolved during further electrochemical treatment see below).

On the XPS spectrum of Pt 4*f* (not shown), the presence of Cu 3*p* peaks is not seen as it was observed before [32]. This means that the Pt shell is compact enough and metallic Cu is recessed into the core of the material. At the same time, no shift of Pt XPS peaks could be confirmed: The observed BEs are very close to the reference ones of bulk Pt, BE for $4f_{7/2}$ 71.0 eV was found instead of 71.1 eV and for $4f_{5/2}$ 74.3 eV was determined instead of 74.4 eV. Note, however, that, as also discussed before [35, 41], metal–metal electronic interactions in alloy or hybrid bimetallic systems are only expected to result in clear XPS peak shifts in the case of homogeneous alloys and not for heterogeneous systems (e.g., core–shell arrangements or near-surface alloys [42].

3.2 Electrochemical characterization

Figure 4 shows the resulting cyclic voltammograms, CVs, (at 50 mV s^{-1} potential scan rate) of a Pt(Cu)/C (18.5 % w/w Pt, 0.5 mg cm^{-2} Pt loading) coated glassy carbon electrode after repetitive scanning in deaerated 0.1 M $HClO_4$ solutions between hydrogen and oxygen evolution. For comparison, the similar voltammogram of a Pt/C ETEK (20 % w/w Pt, 0.5 mg cm^{-2} Pt loading) coated electrode is also shown in the Inset. It can be seen that the stabilized voltammogram of the Pt(Cu)/C electrode resembles that of polycrystalline Pt (hydrogen adsorption/desorption peaks and oxide formation/stripping wave/peak), indicating that the remaining Cu particles are covered (protected) by Pt, whereas any originally present on the surface has been dissolved by anodic or transpassive dissolution and that Pt is the only electroactive species present on the surface. The electrochemically active surface areas (ECSAs) were calculated from the hydrogen adsorption/desorption region, taking into account that the charge associated with the formation or stripping of a hydrogen monolayer is 210 μC cm^{-2} [43]. The ill-defined hydrogen adsorption/desorption envelope is typical for Pt nanoparticles supported on carbon powders and bound with the Nafion® ionomer, where high capacitive currents are observed due to the carbon support. The estimated roughness factors (Pt electroactive surface area per electrode substrate geometric area) and ECSAs, based on Pt loadings (mass-specific electroactive area), were 42 cm^2 cm^{-2} and 8.4 m^2 g^{-1} for Pt(Cu)/C; for Pt/C ETEK, they were estimated to be 86 cm^2 cm^{-2} and 17.2 m^2 g^{-1}, respectively.

The rather low values of mass-specific areas could be attributed to particle aggregation, polymer blocking and details of film preparation. For relatively high Pt loadings (0.5–3 mg cm^{-2}) and Nafion® contents (>30 % w/w), as is the case of our coatings, a lowering of mass-specific areas has been reported [44, 45]. We should note that the electroactive areas reported here are only used for comparison of the electrocatalytic activity of the electrodes. The small ECSA value for the Pt(Cu)/C catalyst can be due to the greater trend of Pt(Cu) particles to aggregation (see the TEM micrographs above). Consequently, part of Pt surface area could be inaccessible and result in low catalyst utilization.

Figure 5 presents the first cycle of CVs in a nitrogen-purged acid solution, following CO adsorption at +0.10 V in the CO-saturated solution for Pt(Cu)/C and Pt/C ETEK. The oxidation peak in the 0.4–0.8 V range corresponds to the oxidative stripping of a preadsorbed CO monolayer. There is significant negative shift of the CO oxidation peak from ca +0.6 V for Pt/C to ca +0.5 V for Pt(Cu)/C. This finding indicates the easier electro-desorption of CO from the modified Pt(Cu) electrode, either due to a weakening of the Pt–CO bond or/and an increase in its oxidation rate by adsorbed O species [13, 32]. Note that this 100 mV shift was larger than that observed for Pt(Cu) catalysts prepared by a chemically deposited Cu precursor (ca 50 mV shift in [32]), suggesting that in the prepared material the Pt–Cu interactions were tuned better for CO oxidation. Also, this significant negative shift should be contrasted to no shift observed in the case of Pt(Ni) catalysts [35].

3.3 Methanol oxidation

Figure 6 presents the positive-going potential sweep voltammograms (at 5 mV s^{-1} potential scan rate) of Pt(Cu)/C and Pt/C coated glassy carbon electrodes in deaerated 0.1 M $HClO_4$ + 0.5 M MeOH solutions. The currents were normalized by Pt electroactive surface areas (j_e), calculated from the H adsorption/desorption region, and specific activities of the catalysts were compared. One can see that the Pt(Cu)/C electrodes have moderately superior specific catalytic activity for MOR than the commercial Pt/C catalyst, even at polarizations lower than +0.4 V which are relevant to fuel cell operation. The more pronounced intrinsic catalytic activity of the Pt(Cu)/C material when

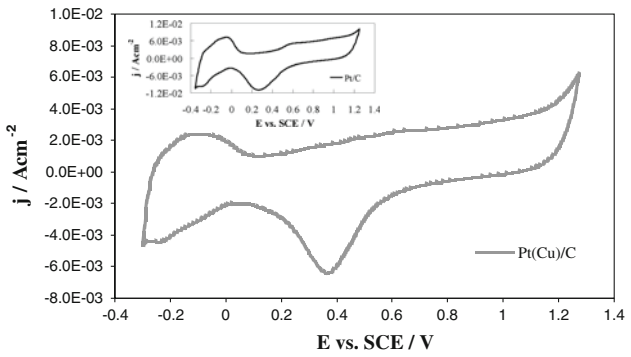

Fig. 4 Cyclic voltammograms (at 50 mV s^{-1} potential scan rate) of Pt(Cu)/C coated glassy carbon electrode in deaerated 0.1 M $HClO_4$ solutions. Inset: CV of Pt/C ETEK electrode

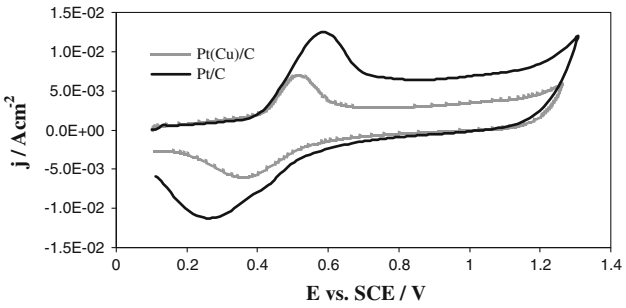

Fig. 5 Voltammograms (at 50 mV s^{-1} potential scan rate) of Pt(Cu)/C and Pt/C ETEK coated glassy carbon electrodes in a deaerated 0.1 M $HClO_4$ solution, following CO adsorption at +0.10 V versus SCE in the CO-saturated solution

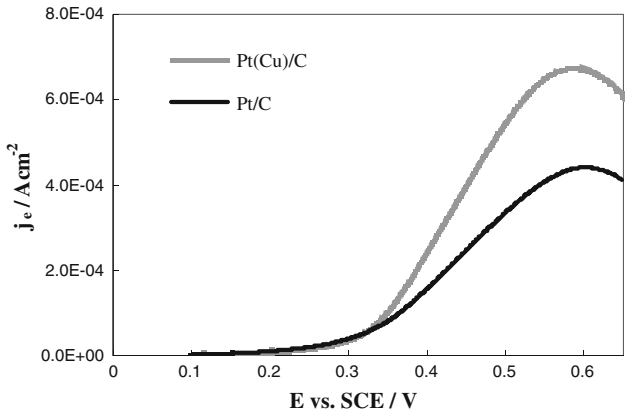

Fig. 6 Positive-going potential sweep voltammograms (at 5 mV s^{-1} potential scan rate) of Pt(Cu)/C and Pt/C coated glassy carbon electrodes in deaerated 0.1 M $HClO_4$ + 0.5 MeOH solutions. The currents are normalized by Pt electroactive surface area (j_e)

compared to Pt/C catalyst can be interpreted by the modification of the electronic properties of Pt by Cu and its optimum effect on methanol oxidative chemisorptions and CO oxidative removal, as interpreted by means of d-band center energy modifications in our previous works [27, 32, 35]. The intrinsic catalytic activity at low overpotentials of the Pt(Cu)/C material prepared from electrolessly deposited Cu precursors seems to be higher than that of both Pt(Ni) prepared form electrolessly deposited Ni and Pt(Cu) prepared from chemically formed Cu. Also, the activity of our catalysts is higher than that of those prepared in a similar manner in References [29–31]; this is presumably due to the lower Cu content of those catalysts (and hence decreased Pt–Cu interactions and associated Pt modification effects).

Figure 7 shows the same results of Fig. 6 but with currents normalized by mass of Pt in the catalyst (j_m). The

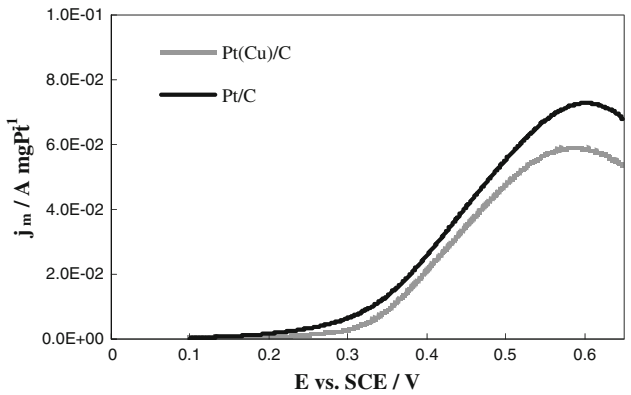

Fig. 7 Positive-going potential sweep voltammograms (at 5 mV s^{-1} potential scan rate) of Pt(Cu)/C and Pt/C coated glassy carbon electrodes in deaerated 0.1 M $HClO_4$ + 0.5 MeOH solutions. The currents are normalized by mass of Pt in the catalyst (j_m)

comparison of the mass activity of the catalysts is of practical importance in view of the fact that this parameter incorporates catalytic activity, surface area and structure-utilization effects. At about +0.4 V, the mass activities of Pt(Cu)/C and Pt/C are 2.1×10^{-2} and 2.6×10^{-2} A $mgPt^{-1}$, respectively. The fact that the Pt(Cu)/C of this work, despite its higher intrinsic activity, shows comparable mass-specific activity to that of a commercial Pt/C results from its lower surface area, associated with its higher degree of aggregation (as depicted in the TEM micrographs) and also confirmed by the lower ECSA values estimated.

4 Conclusions

1. Pt(Cu) catalyst powders were prepared on high surface area carbon supports by a combination of electroless deposition of Cu on C and subsequent partial galvanic replacement of deposited less noble metal by Pt.
2. XRD characterization of the thus prepared Pt(Cu)/C catalysts has shown the formation of Pt–Cu alloys. EDS, XRD and XPS results and the electrochemical characterization of the materials indicate that Pt(Cu) particles consisted of a Pt outer shell, a Pt-rich alloy Pt–Cu in the interior (70 at.% Pt–30 at.% Cu and very small pockets Cu in the core.
3. The Pt(Cu)/C catalysts prepared from electrolessly deposited Cu precursors have the highest intrinsic catalytic activity for methanol oxidation at low overpotentials among similar Pt(Cu)/C and Pt(Ni)/C materials reported recently and commercial Pt/C catalysts.
4. An additional advantage of the Pt(Cu)/catalysts of this work with respect to all the above-mentioned catalysts is their high activity for CO oxidation which may prove useful for CO poison tolerance during long term direct methanol fuel cell operation.
5. Additional advantages of the Pt(Cu)/catalysts of this work with respect to the Pt(Cu)/C catalyst of [32] (whereby Cu was chemically formed) are that it contains a Pt quantity (18.5 vs. 10 % w/w) comparable to that of commercial catalysts and that its preparation is associated with smaller Cu losses due to competitive to platinization reactions (18 % vs. 72 % Cu precursor losses).
6. As a result of a rather high degree of agglomeration, the Pt(Cu)/C material of this work has inferior mass-specific activity than the above-mentioned Pt(Cu)/C and Pt(Ni)/C materials but still comparable to that of commercial Pt/C catalysts. A modification of the size and properties of the electrolessly deposited Cu precursor particles should be sought so that the resulting Pt(Cu) particles acquire an optimum size.

Acknowledgments This research has been co-financed by the European Union (European Social Fund—ESF) and Greek national funds through the Operational Program "Education and Lifelong Learning" of the National Strategic Reference Framework (NSRF)—Research Funding Program: Heracleitus II. Investing in knowledge society through the European Social Fund. Part of the investigations was made within the framework of bilateral projects for collaboration between Bulgarian Academy of Sciences and Fonds Wetenschappelijk Onderzoek (Belgium) and Bulgarian Academy of Sciences and Wallonie-Bruxelles International (Belgium).

References

1. Arico AS, Srinivasan S, Antonucci V (2001) DMFCs: from fundamental aspects to technology development. Fuel Cells 1:133–161
2. McNicol BD, Rand DAJ, Williams KR (1999) Direct methanol–air fuel cells for road transportation. J Power Sources 83:15–31
3. Lamy C, Lima A, Le Rhun V, Delime F, Coutanceau C, Léger JM (2002) Recent advances in the development of direct alcohol fuel cells (DAFC). J Power Sources 105:283–296
4. Hamnett A (2003) Handbook of Fuel Cells: Fundamentals, Technology and Applications. In: Vielstich W, Lamm A, Gasteiger HA (eds) Direct methanol fuel cells (DMFC). Wiley, Chichester, pp 305–322
5. Jarvi TD, Sriramulu S, Stuve EM (1997) Potential dependence of the yield of carbon dioxide from electrocatalytic oxidation of methanol on platinum (100). J Phys Chem B 101:3649–3652
6. Hogarth MP, Ralph TR (2002) Catalysis for low temperature fuel cells. Platinum Metals Rev 46:146–164
7. Liu Z, Lee JY, Chen W, Han M, Gan LM (2004) Physical and electrochemical characterizations of microwave-assisted polyol preparation of carbon-supported PtRu nanoparticles. Langmuir 20:181–187
8. Li L, Xing Y (2007) Pt–Ru nanoparticles supported on carbon nanotubes as methanol fuel cell catalysts. J Phys Chem C 111:2803–2808
9. Nagle LC, Rohan JF (2008) Aligned carbon nanotube–Pt composite fuel cell catalyst by template electrodeposition. J Power Sources 185:411–418
10. Watanabe M, Motoo S (1975) Electrocatalysis by ad-atoms: Part III. Enhancement of the oxidation of carbon monoxide on platinum by ruthenium ad-atoms. J Electroanal Chem 60:275–283
11. Ishikawa Y, Liao M-S, Cabrera CR (2000) Oxidation of methanol on platinum, ruthenium and mixed Pt–M metals (M = Ru, Sn): a theoretical study. Surf Sci 463:66–80
12. Hammer B, Nørskov JK (2000) Theoretical surface science and catalysis—calculations and concepts. Adv Catal 45:71–129
13. Kitchin JR, Nørskov JK, Barteau MA, Chen JG (2004) Modification of the surface electronic and chemical properties of Pt(111) by subsurface 3*d* transition metals. J Chem Phys 120:10240–10246
14. Antolini E, Salgado JRC, Gonzalez ER (2006) The methanol oxidation reaction on platinum alloys with the first row transition metals: the case of Pt–Co and –Ni alloy electrocatalysts for DMFCs: A short review. Appl Catal B: Env 63:137–149
15. Antolini E (2007) Platinum-based ternary catalysts for low temperature fuel cells: Part I. Preparation methods and structural characteristics. Appl Catal B: Env 74:324-336; Part II. Electrochemical properties. Appl Catal B: Env 74:337–350
16. Antolini E, Lopes T, Gonzalez ER (2008) An overview of platinum-based catalysts as methanol-resistant oxygen reduction materials for direct methanol fuel cells. J Alloys Compd 461:253–262
17. Jayasayee K, Rob Van Veen JA, Manivasagam TG, Celebi S, Hensen EJM, Bruijn FA (2012) Oxygen reduction reaction (ORR) activity and durability of carbon supported PtM (Co, Ni, Cu) alloys: influence of particle size and non-noble metals. Appl Catal B: Env 111–112:515–526
18. Bonnemann H, Brijoux W, Brinkmann R, Dinjus E, Jouben T, Korall B (1991) Formation of colloidal transition metals in organic phases and their application in catalysis. Angew Chem Int Ed Engl 30:1312–1314
19. Wang Y, Ren J, Deng K, Gui L, Tang Y (2000) Preparation of tractable platinum, rhodium, and ruthenium nanoclusters with small particle size in organic media. Chem Mater 12:1622–1627
20. Adzic R, Zhang J, Sasaki K, Vukmirovic M, Shao M, Wang J, Nilekar A, Mavrikakis M, Valerio J, Uribe F (2007) Platinum monolayer fuel cell electrocatalysts. Top Catal 46:249–262
21. Brankovic SR, Wang JX, Adzic RR (2001) Metal monolayer deposition by replacement of metal adlayers on electrode surfaces. Surf Sci 474:L173
22. Van Brussel M, Kokkidinis G, Vandendael I, Buess-Herman C (2002) High performance gold-supported platinum electrocatalyst for oxygen reduction. Electrochem Commun 4:808–813
23. Van Brussel M, Kokkidinis G, Hubin A, Buess-Herman C (2003) Oxygen reduction at platinum modified gold electrodes. Electrochim Acta 48:3909–3919
24. Papadimitriou S, Tegou A, Pavlidou E, Kokkinidis G, Sotiropoulos S (2008) Preparation and characterisation of platinum- and gold-coated copper, iron, cobalt and nickel deposits on glassy carbon substrates. Electrochim Acta 53:6559–6567
25. Tegou A, Papadimitriou S, Kokkinidis G, Sotiropoulos S (2010) A rotating disc electrode study of oxygen reduction at platinised nickel and cobalt coatings. J Solid State Electrochem 14:175–184
26. Papadimitriou S, Armyanov S, Valova E, Hubin A, Steenhaut O, Pavlidou E, Kokkinidis G, Sotiropoulos S (2010) Methanol oxidation at Pt–Cu, Pt–Ni, and Pt–Co electrode coatings prepared by a galvanic replacement process. J Phys Chem C 114:5217–5223
27. Tegou A, Papadimitriou S, Mintsouli I, Armyanov S, Valova E, Kokkinidis G, Sotiropoulos S (2011) Rotating disc electrode studies of borohydride oxidation at Pt and bimetallic Pt–Ni and Pt–Co electrodes. Catal Today 170:126–133
28. Ammam M, Easton EB (2013) PtCu/C and Pt(Cu)/C catalysts: synthesis, characterization and catalytic activity towards ethanol electrooxidation. J Power Sources 222:79–87
29. Podlovchenko BI, Gladysheva TD, Filatov AY, Yashina LV (2010) The use of galvanic displacement in synthesizing Pt(Cu) catalysts with the core-shell structure. Russ J Electrochem 46:1189–1197
30. Podlovchenko BI, Krivchenko VA, Maksimov YM, Gladysheva TD, Yashina LV, Evlashin SA, Pilevsky AA (2012) Specific features of the formation of Pt(Cu) catalysts by galvanic displacement with carbon nanowalls used as support. Electrochim Acta 76:137–144
31. Podlovchenko BI, Gladysheva TD, Krivchenko VA, Maksimov YM, Filatov AY, Yashina LV (2012) Effect of copper deposit morphology on the characteristics of a Pt(Cu)/C-catalyst obtained by galvanic displacement. Mendeleev Commun 22:203–205
32. Mintsouli I, Georgieva J, Armyanov S, Valova E, Avdeev G, Hubin A, Steenhaut O, Dille J, Tsiplakides D, Balemenou S, Sotiropoulos S (2013) Pt–Cu electrocatalysts for methanol oxidation prepared by partial galvanic replacement of Cu/carbon powder precursors. Appl Catal B: Env 136–137:160–167
33. Wang X, Wang H, Wang R, Wang Q, Lei Z (2012) Carbon-supported platinum-decorated nickel nanoparticles for enhanced methanol oxidation in acid media. J Solid State Electrochem 16:1049–1054
34. Hu Y, Shao Q, Wu P, Zhang H, Cai C (2012) Synthesis of hollow mesoporous Pt–Ni nanosphere for highly active electrocatalysis

toward the methanol oxidation reaction. Electrochem Commun 18:96–99
35. Mintsouli I, Georgieva J, Valova E, Armyanov S, Kakaroglou A, Hubin A, Steenhaut O, Dill J, Papaderakis A, Kokkinidis G, Sotiropoulos S (2013) Pt–Ni carbon-supported catalysts for methanol oxidation prepared by Ni electroless deposition and its galvanic replacement by Pt. J Solid State Electrochem 17: 435–443
36. Ando Y, Sasaki K, Adzic RR (2009) Electrocatalysts for methanol oxidation with ultra low content of Pt and Ru. Electrochem Commun 11:1135–1138
37. Georgieva M, Petrova M, Dobrev D, Velkova E, Stoychev D (2011) Chemical deposition of composite copper—diamond coatings on non-metallic substrate. Mater Plastice 48: 269–272
38. Lovrecek B, Mekjavic I, Metikos-Hukovic M (1985) Standard Potentials in Aqueous Solution. In: Bard AJ, Parsons R, Jordan J (eds) Bismuth, Marcel Dekker, Inc, NY and Basel
39. Cullity ED, Stock SR (2001) Elements of X-ray diffraction. 3rd edn, Prentice-Hall Inc, pp 167–171
40. Xu H-C, Seshadri G, Kelber JA (2000) Effect of sulfur on the oxidation of copper in aqueous solution. J Electrochem Soc 147:558–561
41. Teng X, Du W, Wang Q (2011) Nanowires—fundamental research. In: Hashim A (ed) Synthesis of Pt–containing metals alloy and hybrid nanowires and investigation of electronic structure using synchrotron-based X-ray absorption techniques, InTech, open access at http://www.intechopen.com/books/nanowires-fundamental-research
42. Greeley J, Mavrikakis M (2006) Near-surface alloys for hydrogen fuel cell applications. Catal Today 111:52–58
43. Bagotzky VS, Vassilyev YB (1967) Mechanism of electro-oxidation of methanol on the platinum electrode. Electrochim Acta 12:1323–1343
44. Choi SM, Kim HJ, Jung JY, Yoon EY, Kim WB (2008) Pt nanowires prepared via a polymer template method: its promise toward high Pt-loaded electrocatalysts for methanol oxidation. Electrochim Acta 53:5804–5811
45. Pozio A, De Francesco M, Gemmi A, Cardellini F, Giorgi L (2002) Comparison of high surface Pt/C catalysts by cyclic voltammetry. J Power Sources 105:13–19